Tolerable ELMs in Conventional and Advanced Scenarios at ASDEX Upgrade

O. Gruber, S. Günter, A. Herrmann, L.D. Horton, P.T. Lang, M. Maraschek, S. Saarelma[+], A.C. Sips, J. Stober, W. Suttrop, H. Zohm and the ASDEX Upgrade Team

Max-Planck-Institut für Plasmaphysik, EURATOM Assoc., D-85748 Garching, Germany
[+] Helsinki University of Technology, EURATOM-Tekes Assoc., Espoo, Finland

e-mail contact of main author: gruber@ipp.mpg.de

Abstract. Recent ASDEX Upgrade experiments have integrated benign type II ELMs exhibiting tolerable peak heat loads on the target plates with high plasma performance in terms of confinement, beta, and density. In both conventional and advanced H-modes, the operation window with type II ELMs was extended down to $q_{95} \approx 3.5$ in close to double null configurations at sufficiently high edge pedestal density above 50% of the Greenwald density. Type I ELMs are suppressed at almost constant pedestal parameters and confinement levels, presumably due to a change in edge stability provided by higher edge magnetic shear. Since conventional reactor designs are optimised at $q_{95} \approx 3$, operation with type II ELMs has to compensate the required higher q-value by enhanced performance. This was achieved in H-mode scenarios with high $\beta_N > 3.5$, improved confinement ($H_{98\text{-}P} \approx 1.3$), and averaged densities of 90% of Greenwald density allowing for type II ELMs. In this integrated scenario with a high triangular plasma shape the confinement is improved via peaked density profiles. Active triggering and mitigation of type I ELMs by means of hydrogen pellet injection was demonstrated with enhancement of the ELM frequency to the pellet rate of 20 Hz. The enhanced D_α (EDA) mode was not reproducible at ASDEX Upgrade.

1. Introduction

The reference scenario for ITER inductive operation with Q≈10 is the ELMy H-mode. Besides sufficient confinement (H-mode confinement of $H_{H98\text{-}P} = 1$) and stability margin (in terms of beta normalised $\beta_N \approx 2$) at low $q_{95} \approx 3$, operation at a density close to the Greenwald density n_{GW} for optimised heat and particle exhaust and ELMs (edge localised modes) producing tolerable peak heat loads at the divertor targets are needed in an integrated scenario. Type I ELMs are normally connected with the best performing H-modes but result in pulsed heat flows to the divertor target plates which would cause high erosion and severely reduce the lifetime of the divertor in ITER FEAT to unacceptable levels [1,2].
Each ELM expels energy from the plasma edge on a sub-millisecond time scale, which in ASDEX Upgrade type I ELMy H-modes leads to peak divertor power loads of up to 60 MW/m^2 at the inner target in Div IIb in contrast to average loads below 5 MW/m^2. In time average, the energy transported by transient ELM events is up to 30% of the total energy deposited in the divertor (with no significant broadening compared to the profiles between ELMs) [3]. Extrapolations for ITER result in power loads of > 1 GW/m^2 [2]. The limit for transient heat loads is given by the maximum tolerable surface temperature before ablation or melting of the surface. Therefore the product of power flux and square root of event time must be kept below a material dependent limit, i.e. the tolerable amount of energy deposited with a heat pulse, ΔW_{div}, is increasing with square root of deposition time Δt and the wetted area

$$\Delta W_{div} / (\Delta t^{1/2} A_{div}) < 20 \text{ MJm}^{-2}\text{s}^{-1/2} \quad \text{for CFC graphite [3].}$$

These values are already achieved with giant ELMs in JET despite techniques for heat flux reduction such as the increase of wetted area by proper geometric orientation and poloidal flux expansion as well as impurity radiation. The required limit for ITER for the amount of energy lost by an ELM normalised to the plasma energy is $\Delta W_{ELM}/W_p < 1\%$ [2].
The energy lost by an ELM is described by different scalings based either on the pedestal collisionality or on a parallel transport limit to the divertor depending on the ratio of ELM duration and parallel ion transit time as calculated from the pedestal temperature (plugging model) [1,2]. These models predict an ITER level of $\Delta W_{ELM}/W_p < 4\%$ or $\Delta W_{ELM} < 22$ MJ [1]. The scaling of ELM duration with machine size is then essential to predict the ELM load on the ITER divertor. Taking into account the variability of ELM size, the fraction of energy

arriving at the target plates which is about constant in ASDEX Upgrade and JET ($\Delta W_{div}/\Delta W_{ELM} \geq 0.5$), the ELM asymmetry between inner and outer target (≈1-2) and the small strike zone broadening, even the best case estimates for ELM impact in ITER are above the ablation limit. Empirically, it is observed that the fraction of type I ELM transported power is constant, $f_{ELM}\,\Delta W_{ELM} / P_{heat} \approx 0.2$ (JET, DIII-D, ASDEX Upgrade), leading to a scaling $\Delta W_{ELM}/W_p \approx 0.2 / (f_{ELM}\,\tau_E)$. Thereby the normalised ELM energy losses increase with machine size (see FIG. 6), which can be explained by the fact that the ELM frequency, f_{ELM}, decreases faster than the energy confinement time increases: $f_{ELM} \propto \tau_E^{-1.7}$ [3]. This empirical scaling predicts for ITER a much higher ELM energy loss than given by the above models.
In addition to the energy exhaust problem the sustainment of strong internal transport barriers needed for high bootstrap current drive and hence a possible stationary non-inductive tokamak operation is limited by the occurrence of type I ELMs [4]. Type III ELMs show a potential to strongly reduced heat loads but they lead to reduced performance in terms of confinement and β. On the other hand ELMs can help to limit impurity influx. Therefore, the control of ELM behaviour and the development of operation scenarios with tolerable ELMs preserving high performance is required.
The following sections report on recent progress made in ASDEX Upgrade experiments on alternative ELM scenarios allowing adequate power handling both in conventional and advanced H-modes since the last IAEA conference [5]. High shaping capability with elongations $\kappa \leq 1.8$ and triangularities $<\delta>$ of up to 0.45 (top/bottom averaged at the separatrix) with adjusted divertor geometry allowed the study of the influence of plasma shape on ELM behaviour and operational limits. Especially type II ELMs combine the good performance of the type I ELM regime with reduced peak heat loads below 10 MW/m^2 as seen with type III ELMs [6,7,8,9,10,11]. The integration of benign type II ELMs in steady-state advanced scenarios with enhanced performance could be demonstrated. Dimensionless ELM scaling experiments were done as well as tests of the reproducibility of other small ELM regimes such as the enhanced D_α (EDA) mode [12,13] or the ELM-free quiescent H-mode (QH) [14] (results are given in [15]). Additionally, active type I ELM control by means of shallow hydrogen pellet or impurity injection (carbon laser blow-off) was started [16].

2. Tolerable type II ELMs close to the Greenwald density

On ASDEX Upgrade small irregular high-frequency type II ELMs were identified, partly mixed with type I ELMs, for $q_{95} > 4.2$ and $\delta > 0.4$ close to a double null configuration, but in contrast to experiments reported earlier [6,7] at high densities close to the Greenwald limit [5,8,9,10,11]. As they preserve high edge pressures, the confinement is almost as good as with type I ELMs and significantly higher than for type III ELMs, providing $\tau_E/\tau_{H98\text{-}P} \approx 1$. In recent conventional H-mode experiments steady-state type II ELM phases could be established, limited only by the length of the current flattop phase. The type II ELM features are as described earlier: The ELM amplitude of the D_α signal decreases, and ELM frequencies between 0.5 and 1 kHz are observed. Even in the case of non-conclusive D_α traces, magnetic precursors and target plate thermography allow a clear identification. Magnetic measurements close to the separatrix and reflectometry show that single type II ELMs, best observed in mixed type I and II phases, are characterised by a precursor of broadband MHD fluctuations in the frequency range between 15 and 30 kHz [9]. Correlation analyses of poloidal and toroidal arrays of magnetic pick-up coils give mode numbers $m \geq 14$, $n \approx 3\text{-}4$, which corresponds to the localisation at the plasma edge. In pure type II ELM phases the precursors unify to a wide frequency band. New features were detected from magnetic coils on the low field side with a high frequency response up to 1 MHz and sampled at 2.5 MHz [17]. While type I ELMs exhibit a high frequency precursor around 400 kHz with a local $m \approx 10\text{-}15$ at the outer midplane 1-2 ms before the actual ELM, type II ELMs show a broadband fluctuation around 700-800 kHz. The thermography data of the divertor target plates show that the peak power load is strongly reduced with type II ELMs, especially at the inner target. The power flux on the plates is quasi-stationary and slightly above the value in between ELMs in purely type I ELM phases (FIG. 1).
The condition for type II ELMs in terms of q_{95}, triangularity, closeness to double null and density was extensively studied. In single discharges at constant gas puff rate, normalised $n_e/n_{GW} \approx 0.9$ and nearly constant normalised confinement time H-98P(y) only a tendency for a necessary closer DN operation at lower triangularities $<\delta> \approx 0.35$ was seen. The necessary

difference between the active and passive separatices varies between 5 mm ≤ Δx_p ≤ 20 mm at the outer midplane (error ± 5 mm). Ramp-up of the density at fixed geometry (Δx_p = 5 mm) via gas puffing leads to the appearance of type II ELMs between 0.85 and 0.95 times n_{GW} and finally to the transition to type III ELMs at the Greenwald density with reduced confinement. On the other hand, density ramp-down shows the reappearance of type I ELMs at lower densities below 80% of n_{GW}. The transition to type II ELMs is not abrupt; they appear in between type I ELMs or vice versa. Even at $\langle\delta\rangle \approx 0.3$, not close to double null, type II ELMs can be found. If type II ELMs appear they build up in frequency and amplitude till the next type I ELM is triggered, so the time in between the type I ELMs is increased compared to intervals without type II ELMs [8]. Then the time between type I ELMs fills up with the irregular type II ELMs and the type I ELMs become small, and finally the transition to only small ELMs occurs. FIG. 2 shows the ELM transitions with increasing shaping and density towards double null.

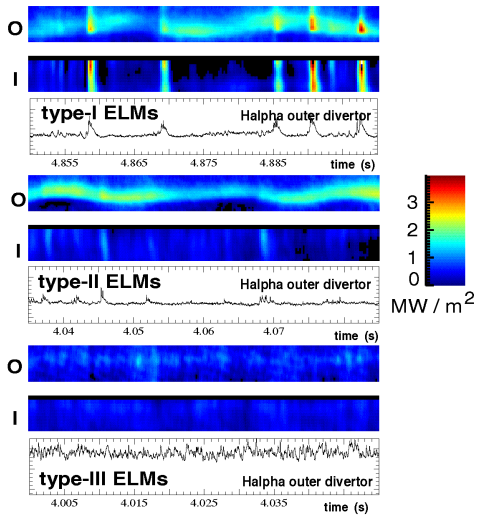

FIG. 1 Heat fluxes to the outer (o) and inner (i) strike point regions from infrared thermography for type I, II and III ELMs. The height of each bar corresponds to a poloidal length of 7 cm along the target surface

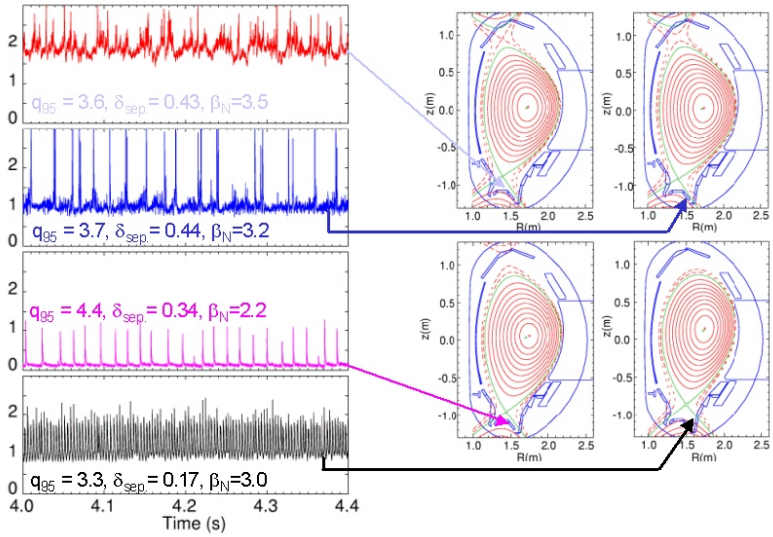

FIG. 2: ELM type behaviour in different H-mode discharges indicated by the D_α signal from the outer lower divertor. Increasing shaping at n_e/n_{GW} = 0.5 leads first to an increase in type I ELM size with high transient heat loads and then at higher densities, $n_e/n_{GW} \approx 0.85$, and towards a double null mixed type I/type II phases and finally continuous type II ELMs are obtained (from bottom to top).

3. Integrated high performance scenario with tolerable type II ELM activity

The integration of benign type II ELMs in steady-state advanced H-modes with enhanced performance in terms of beta, confinement and plasma densities extends the "improved H-mode" scenario reported earlier [5,18,19]. Performance expressed in terms of beta normalised β_N = 2.6 and confinement improvement above H-mode of $H_{98\text{-}P}$ = 1.7 at modest triangularity of $\langle\delta\rangle$ = 0.3 had already been obtained, with ASDEX Upgrade records in the triple product $n_i(0)\, T_i(0)\, \tau_E = 1 \cdot 10^{20}$ m^{-3} keV. The plasma density of <50% of the Greenwald density in these discharges resulted in low collisionality, but had neither adequate divertor performance nor tolerable ELMs. Recent experiments have concentrated on a steady state "high-β_N H-mode" scenario with the aim to maximise both β_N and confinement by pressure and current profile control and by increasing the triangularity up to 0.45 and to raise the density to get reactor compatible divertor loads [10]. Such an advanced performance is most probably needed with type II ELM operation in ITER to compensate for the required higher q_{95} value being above 3 up to now (see above and Sect. 4).

At highly shaped plasma configurations with $\langle\delta\rangle$ = 0.42, near double null, high-β_N H-mode discharges with $\beta_N > 3.5$ and good confinement $H_{98\text{-}P} \approx 1.3$ have been obtained in steady state at $q_{95} \approx 3.6$, with $\beta_N H_{89\text{-}P}$ reaching up to 8.0 for 40 energy confinement times [11,15]. In transient conditions, $\beta_N H_{89\text{-}P}$ = 11.5 has been obtained limited by neo-classical tearing modes (NTMs). In these discharges line averaged densities of 80%-90% of the Greenwald density are

achieved while maintaining the good confinement. In both advanced scenarios, the improved and the high-β_N H-modes, weak central magnetic shear and q(axis) close to 1 are observed, with the sawteeth replaced by fishbones, reducing the seed for the limiting NTMs. The temperature profiles are still stiff with the gradient length governed by ITG and TEM turbulence, while the confinement is improved via peaked density profiles [19,20]. Based on the common underlying physics the operational regimes of these advanced H-mode scenarios have been merged in terms of triangularity and density and extended towards $q_{95} \approx 3.2$. Both β_N and H factors increase with triangularity [11,15], but do not depend on q values over a range of $q_{95} = 3.2\text{-}4.5$ [11]. Even in the presence of NTMs still β_N values of 3 could obtained in stationary discharges at high densities. To avoid both NTMs, which are enhanced by peaked density profiles driving more bootstrap current, as well as increasing impurity content a careful density profile control by gas puffing, on/off-axis tangential NBI deposition and central ICRH deposition is an essential element. Non-inductive current drive is up to 60% relying on bootstrap and NBI driven currents.

At the highest densities and close to double null configurations a strong reduction of the ELM activity to type II ELMs is observed as in conventional H-modes, providing a strong reduction of the peak heat load on the divertor which becomes steady in the range of 6 MW/m^2, despite the high input power used (≥10 MW). In the discharge shown in FIG. 3 the line averaged electron density rises slowly to $9.1 \cdot 10^{19}$ m^{-3}. Measurement of the density by 5-channel DCN interferometry, Thomson scattering and reflectometry show an pedestal top density of 6-$7 \cdot 10^{19}$m^{-3}. During the NBI heating phase, the ELMs are reduced significantly in size as the density increases and the plasma configuration is moved up, closer to a double null configuration. This movement to a double null configuration is made deliberately and is completed at 3.2 s. Infrared data of Fig. 3 show that initially type I ELMs are observed on the outer target with a peak heat flux of up to 18 MW/m^2 (at about 2 s). The type I ELM activity drops and finally (between 3.5 and 5.6 s) the maximum heat flux on the divertor has become steady, in the range of 6 MW/m^2, and only type II ELMs remain. For the inner target plate, high peak loads are observed during type I ELMs, however, the heat flow reduces to nearly zero during the close to double null configuration phase. During the transition and in the type II phase the time averaged heat flux to the outer divertor does not change. This behaviour is very

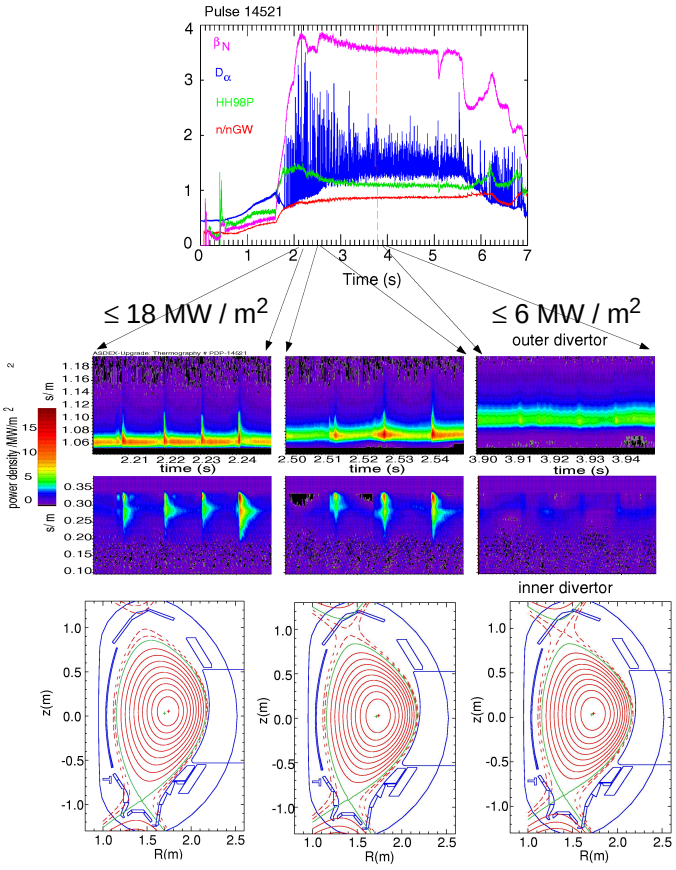

FIG. 3: Performance parameters of an advanced H-mode discharge and detailed overview of the ELM activity heat fluxes to the outer and inner divertor targets from infrared thermography for three time intervals together with the corresponding equilibria. The vertical axis in the IR pictures is the distance along the vertical cross section of the targets, starting from the high field side with the inner divertor.

similar to what is observed for type II ELMs in standard H-mode discharges at medium heating power. Here type II ELMs are achieved despite the high heating powers of ≥10 MW well in excess (factor 5) of the H-mode power threshold and the high gas fuelling rates.
These ASDEX Upgrade results emphasise that at high triangularity enhanced confinement and stability, high β_N, densities close to the Greenwald density allowing cold divertor operation and non-inductively driven currents exceeding 50% of the plasma current can be achieved simultaneously. These aspects combined with tolerable Type II ELMs at $q_{95} > 3.5$ and close to a double-null configurations make this advanced H-modes a serious candidate for a steady state integrated reactor scenario.

4. Pedestal parameters and operational regime of type II ELMs

The operational space and the edge parameter regime for the occurrence of type II ELMs are the same for conventional and advanced H-modes: a combination of closeness to double null and high density. The closeness of the two separatrices is stringent and has to be kept below 1 – 2 cm in the torus midplane as is seen in FIG. 4b. Triangularity or q_{95} are not the decisive parameters, indeed they can vary over a broad range (see FIG. 4). But in experiments on ASDEX Upgrade the close to double null condition is difficult to separate from high triangularity because of the reactor relevant PF coils being outside the TF magnet and distant from the plasma. Consequently the operation space for triangularity could be extended down to top/bottom averaged values of $\langle\delta\rangle = 0.35$ when still operated close to double null. The operation window in q has been extended towards $q_{95} \geq 3.5$ (FIG. 4a) being closer to the ITER reference value. This limit is again connected with the double-null condition due to limitations for the plasma current set by the ASDEX Upgrade poloidal field system and power supplies.
The second condition means a sufficiently high edge pedestal density above 50% of the Greenwald density, which is connected with line averaged densities above 85% of Greenwald density to get type II ELMs. For one given magnetic configuration, the requirement of increasing density to change from type I to type II ELMs can of course be framed as a collisionality limit at the pedestal and has led to the concern, that with the low edge collisionality in ITER type II ELMs might be inaccessible. However, type I ELMs have been observed in discharges with higher collisionality than for type II discharges ($\nu^* \approx 0.3$–2), although in slightly different configurations (see below) [21]. To keep this edge condition, which is in terms of the density required anyway to achieve a "cold" divertor for low enough power fluxes in between ELMs, the gas fuelling rate has to be adjusted to changes in the heating power according to the changing particle transport.
Type I ELMs are suppressed at almost constant pedestal top parameters and pressure gradients. The sustained edge pressures also explain that at stiff temperature gradient length governed by ITG and TEM turbulence the confinement is comparable to the type I ELM regime, while with type III ELMs occurring at reduced edge temperatures and pressures the confinement is reduced. The ELM type changes presumably due to a change in edge stability provided by the increased edge magnetic shear close to double-null. This would also explain that type II ELMs

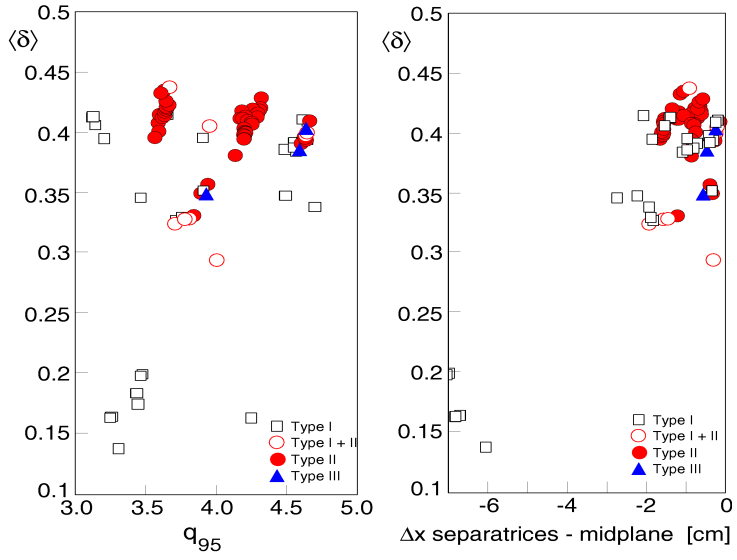

FIG. 4: Operational regime of type I, II and III ELMs in both conventional and advanced scenarios in terms of triangularity δ, q_{95} and the separation Δx_p of the two separatrices in the torus midplane.

are preferentially achieved at higher q(edge) values and that higher β's are supportive. The required high edge densities with connected higher collisionality reduce the edge bootstrap current and correspondingly enhance the edge magnetic shear, supporting the shear argument. The access window for type II ELMs in terms of edge parameters is reduced compared to type I ELMs, but coincides with the reactor relevant domain of high triangular shapes and high density. A combination of reactor relevant high densities and very low edge collisionalities can only be met in ITER.

As an explanation for the type I ELM triggering it was proposed that the plasma edge pressure gradient is at the ballooning limit and then a peeling mode is triggered leading to a high perpendicular energy flux across the separatrix. Recent MHD stability analysis including an estimate for the edge bootstrap current driven by the H-mode edge barrier revealed a change of edge peeling-ballooning instability behaviour for type II conditions compared with type I ELMs [21,22]. The reduced bootstrap current and correspondingly enhanced edge magnetic shear can close the access to the second stability of high-n ballooning modes. This applies to both type I and II ELM regimes at high densities. But the low-n ($n \approx 3$-4) peeling modes, which seem to be responsible for triggering large amplitude type I ELMs in a broad radial edge region [23], are stabilised with the increase in triangularity or magnetic shear as well as the reduced bootstrap current at higher densities. Both described effects lead to the stabilisation of low-n modes and the avoidance of type I ELMs. This is shown in FIG. 5c where the low-n stability of very similar discharges is compared using the GATO code, one with type II ELMs (#15863, $\Delta x_p = 13$ mm) and the other being somewhat less close to double null exhibiting type I and II ELMs at a even slightly higher collisionality (#15865, $\Delta x_p = 26$ mm; see T_e and n_e profiles in FIG. 5a,b). The only unstable edge modes remaining are high-n peeling modes ($n \geq 8$) which can be destabilised even at the lower pressure gradients given by ballooning modes in the first stability region. Their radial extent narrows with increasing n and the eigenfunction becomes more localised towards the edge with higher edge shear (see FIG. 5d), where this localisation effect applies to all mode numbers. Moreover the second X-point creates a strong magnetic shear in its vicinity (as does the first X-point) and eliminates the peeling mode there (see FIG. 5c). The localisation towards the separatrix may lead to small losses of the edge current which are sufficient to linearly stabilise the peeling mode and favours the tendency to smaller amplitudes of the resulting ELMs, consistent with the observed type II ELMs. Also the higher repetition frequency is qualitatively explained by the small amount of edge current to be replaced together with the reduced extent of the ELMing region as well as the tendency for increased resistive diffusion at lower edge temperatures.

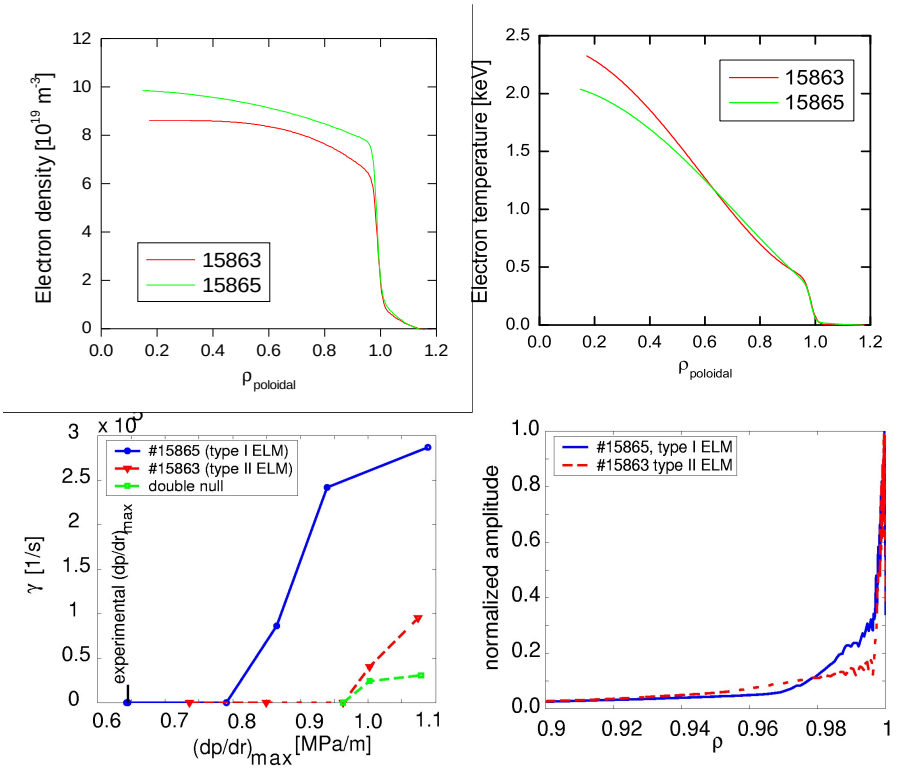

FIG. 5: Electron densities (a) and temperatures (b) for a type I (#15865) and a type II (#15863, closer to double null) ELMy H-mode discharge with otherwise identical parameters.
(c) n=3 peeling mode growth rates as a function of edge pressure gradient for these discharges and for a true double null configuration (shown in green).
(d) Radial envelope of unstable n=8 peeling mode eigenfunctions for these discharges.

5. Alternative ELM regimes and active ELM control

The onset parameters for both type II ELMs and EDA mode are investigated in dedicated comparison experiments between ASDEX Upgrade and Alcator C-Mod [13]. Besides fitting of the dimensionless parameters (ρ*, ν*, β, q) in the plasma core and the shapes a similar heating scenario, namely hydrogen minority heating with matched power and frequency, is used. In close to double null configuration the limited heating power in Alcator C-Mod allowed only matched discharges at 30% lower density and half the heating power compared with that required for type II operation in ASDEX Upgrade. Under these conditions, transient ELM-free or very low frequency type I H-modes are seen in both experiments. With high triangular EDA-mode shapes in ASDEX Upgrade again low frequency type I ELMs are found. The obtained electron collisionality at the pedestal top is 1.4 in ASDEX Upgrade compared with 2.1 in Alcator C-Mod at a density resulting from dimensionless similarity of 60% of Greenwald density. To adjust the collisionality the density was raised by gas puffing in ASDEX Upgrade resulting in enhanced recycling level and type III ELMs. In a second attempt the heating power was reduced leading to L-mode back-transition. Although the EDA mode could not be reproduced on ASDEX Upgrade, a coherent edge MHD activity with a narrow band around 30 MHz in between ELMs was observed. This is reminiscent of the Quasi-coherent mode found at 100±40 kHz in the EDA discharges at Alcator at higher fields[24].

Controlled triggering of type I ELMs by shallow injection of small hydrogen pellets has been successfully demonstrated [16]. Pellets with higher mass used for deep refuelling often cause a burst of ELMs which are stronger than the natural background ELMs. In contrast, each small pellet almost immediately triggers only one ELM such that the ELM frequency was enhanced from the natural rate of 3 Hz in a reference discharge to the pellet rate of 20 Hz at nearly equal density and plasma energy (see FIG. 6). The heating power of 3.8 MW (NI and ICRH) in the reference discharge was just sufficient to enter the type I ELM regime with strong compound ELMs at a low frequency (connected with a short back-transition to the L-mode), while the density was adjusted to the weak pellet refuelling (I_p = 1 MA, B_t = 2 T, q_{95} = 3.8, $<\delta>$ = 0.3). The forced ELM signatures are identical to natural ELMs at the same frequency (20 Hz) and the energy loss / ELM of these forced ELMs agrees with the empirical scaling given in the introduction, $f_{ELM}\,\Delta W_{ELM} / P_{heat} \approx 0.2$ (see FIG. 6). In both reference and controlled discharges the averaged power flux to the targets was equal, but was dispersed in more frequent events in the controlled discharge despite no reduction of the expelled energy per ELM was achieved compared with the empirical scaling. This method may open a route to mitigate the peak heat loads at a given heating power.

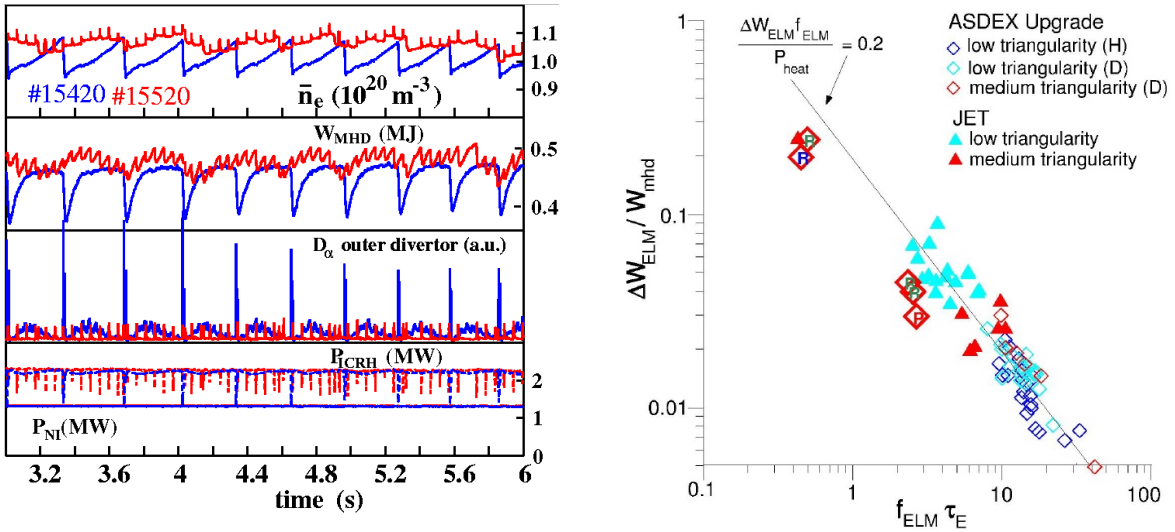

FIG. 6: Controlled type I ELM triggering by pellet injection with a pellet rate of 19 Hz (#15420) and a reference discharge with infrequent compound ELMs (3 Hz). Comparison of the frequency and amplitude of the compound and pellet forced ELMs(◊) with the empirical scaling of type I ELMs [3].

6. Summary and Outlook

H-modes with type I ELMs exhibit the best confinement performance, but the concomitant large power load during the ELM activity may not be acceptable in a reactor. Type III ELMs show nearly no additional heat load on targets, but they entail confinement degradation. Type II ELMy H-modes have been demonstrated on ASDEX Upgrade in both conventional and advanced H-modes for $q_{95} > 3.5$ and $\delta > 0.35$ close to a double null configuration, but in contrast to earlier experiments at high density (absolute or in relation to the Greenwald density) and down to low q values ($q_{95} \geq 3.5$). Type I ELMs are suppressed at almost constant pedestal parameters and pressure gradients, resulting in a similar core confinement with type II ELMs as with type I ELMs. The transition presumably occurs due to a change in edge stability provided by the higher edge magnetic shear close to double-null. Edge MHD measurements and stability calculations point towards a ballooning and high-n peeling mode mechanism.
Advanced H-mode discharges are achieved by the combination of NBI, gas fuelling as well as control of density peaking and impurity content by central ICRH deposition. They maintain high normalised confinement and beta values above the ITER references ($\beta_N H_{89\text{-}P} = 8.0$ for 40 energy confinement times) in combination with line averaged densities of 80%-90% of the Greenwald density necessary for tolerable divertor operation and with almost continuous power losses from the plasma edge without large peak power loads. This new result with low amplitude type II ELMs is maintained even at input powers above 10 MW and is quite attractive for a future reactor. Since conventional reactor designs are optimised at $q_{95} \approx 3$, operation with tolerable type II ELMs has to compensate the required higher q value by advanced performance as achieved in advanced H-modes.
While the ELMless Quiescent H-mode operation – only achievable with counter-NI and at low densities - was reproduced [15], the EDA mode could not be obtained at ASDEX Upgrade. Type I ELM control was demonstrated for the first time by injecting pellets of suitable size. The forced ELMs are comparable to natural ELMs with the same frequency in terms of duration, particle and energy ejection and divertor heat loads. Technical extension towards smaller pellets injected from the low field side to avoid refuelling and higher frequencies are being considered.
Finally, technical enhancements performed presently will prolong the flattop pulse length in ASDEX Upgrade to 10 s for high triangular plasmas allowing the demonstration of steady state conditions over several current diffusion times and will provide triangularities up to 0.55 at reduced currents.

References

[1] Loarte, A., et al., this conference
[2] Frederici, G., et al., Nucl. Fus. **41** (2001) 1967
[3] Herrmann, A., Plasma Phys. Contr. Fusion **44** (2002) 883
[4] Peeters, A., et al., this conference, IAEA-CN-94 EX/P4-03
[5] Gruber, O. et al., Nucl. Fus. **41** (2001) 1369
[6] Ozeki, T., et al., Nucl. Fus. **30** (1999) 1425
[7] Kamada, Y., et al., Plasma Phys. Contr. Fusion **42** (2000) A247
[8] Stober, J., et al., Plasma Phys. Contr. Fusion **43** (2001) A39
[9] Stober, J., et al., Nucl. Fus. **41** (2001) 1123
[10] Sips, A.C.C. et al., Plasma Phys. Contr. Fusion **44** (2002) A151
[11] Sips, A.C.C. et al., accepted for publication in Plasma Phys. Contr. Fusion (2002)
[12] Greenwald, M., et al., Phys. Plasmas **6** (1999) 1943
[13] Suttrop, W., et al., this conference, IAEA-CN-94 EX/P5-07
[14] Greenfield, C.M., et al., Phys. Rev. Letter **86** (2001) 4544
[15] Zohm, H., et al., this conference, IAEA-CN-94 OV/2-1
[16] Lang, P.T., et al., 29th EPS Conf. Plasma Phys. Contr. Fus., Montreux, ECA, **26B** (2002) P-1.038
[17] Maraschek, M., et al., IEA workshop on ELMs, Culham (2002)
[18] Gruber, O., et al., Phys. Rev. Lett. **83** (1999) 1787
[19] Gruber, O., et al., Nucl. Fus. **40** (2000) 1145
[20] Na, Y.-S., et al., Plasma Phys. Contr. Fusion **44** (2002) 1285
[21] Horton, L.D., et al., 29th EPS Conf. Plasma Phys. Contr. Fus., Montreux, ECA, **26B** (2002) P-2.047
[22] Saarelma, S., et al., Nucl. Fus., to be published
[23] Saarelma, S., Günter, S., et al., Plasma Phys. Contr. Fusion **42** (2000) A139
[24] Hubbard, A.E., et al., Phys. Plasmas **8** (2001) 2033